The Egyptian Journal of Remote Sensing and Space Sciences (2016) xxx, xxx–xxx

HOSTED BY

ELSEVIER

National Authority for Remote Sensing and Space Sciences

The Egyptian Journal of Remote Sensing and Space Sciences

www.elsevier.com/locate/ejrs
www.sciencedirect.com

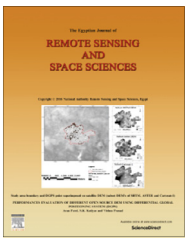

RESEARCH PAPER

Identification of flooded area from satellite images using Hybrid Kohonen Fuzzy C-Means sigma classifier

Krishna Kant Singh [a], **Akansha Singh** [b,*]

[a] *EEE Department, Dronacharya College of Engineering, Gurgaon, India*
[b] *CSE&IT Department, The NorthCap University, Gurgaon, India*

Received 28 February 2016; accepted 28 April 2016

KEYWORDS

KCN;
Remote sensing;
Fuzzy C-Means;
Clustering;
Spectral indices;
PCA

Abstract A novel neuro fuzzy classifier Hybrid Kohonen Fuzzy C-Means-σ (HKFCM-σ) is proposed in this paper. The proposed classifier is a hybridization of Kohonen Clustering Network (KCN) with FCM-σ clustering algorithm. The network architecture of HKFCM-σ is similar to simple KCN network having only two layers, i.e., input and output layer. However, the selection of winner neuron is done based on FCM-σ algorithm. Thus, embedding the features of both, a neural network and a fuzzy clustering algorithm in the classifier. This hybridization results in a more efficient, less complex and faster classifier for classifying satellite images. HKFCM-σ is used to identify the flooding that occurred in Kashmir area in September 2014. The HKFCM-σ classifier is applied on pre and post flooding Landsat 8 OLI images of Kashmir to detect the areas that were flooded due to the heavy rainfalls of September, 2014. The classifier is trained using the mean values of the various spectral indices like NDVI, NDWI, NDBI and first component of Principal Component Analysis. The error matrix was computed to test the performance of the method. The method yields high producer's accuracy, consumer's accuracy and kappa coefficient value indicating that the proposed classifier is highly effective and efficient.

1. Introduction

Natural disasters are major adverse events which result from earth's natural processes. Natural disasters pose a serious threat to life and property, the extent of damage is directly related to the vulnerability of the affected area. The number of occurrences of natural disasters in the last few years has greatly increased. The major disasters include tsunamis, floods, volcanic eruptions, earthquakes etc. Floods are one of the most frequent and devastating natural hazards that occur worldwide. Floods occur due to excessive rainfall in a short duration of time and consequent high river discharge causes a large amount of damage. Flooding results in huge economic losses, destruction of ecological resources, food shortages and starvation of millions of people. Thus one of the major concerns of various countries is to monitor flooding so as to

* Corresponding author.
E-mail addresses: krishnaiitr2011@gmail.com (K.K. Singh), akanshasing@gmail.com (A. Singh).
Peer review under responsibility of National Authority for Remote Sensing and Space Sciences.

http://dx.doi.org/10.1016/j.ejrs.2016.04.003

reduce the effect of floods. In the era of satellites, remote sensing data are used effectively for assessment, identification and management of flood disaster (Manjunath et al., 2007). Traditionally, field surveys or ground inspections were used for damage assessment. The limitation of these methods is that at the time of disaster it becomes difficult to reach the actual site. Remote sensing is a reliable way of providing coverage for wide areas in a cost effective manner and also it overcomes the limitation of surveying the ground in an extreme hydrological event. Satellite images are widely used for monitoring urban expansion and land use cover changes at a medium or large scale, to help better observe and understand the evolution of urbanization and advance the sustainable development process. The application of satellite imagery for flood mapping began with the use of Landsat Thematic Mapper and Multispectral Scanner, the Satellite Pour l'Observation de la Terre (France and Hedges, 1986; Jensen et al., 1985; Watson, 1991; Barton and Bathols, 1989), the Advanced Very High Resolution Radiometer (Gale and Bainbridge, 1994; Rasid and Pramanik, 1993; Sandholt et al., 2003), the Advanced Spaceborne Thermal Emission and Reflection Radiometer (ASTER), MODIS, and Landsat-7 sensors (Brakenridge et al., 2003a,b; Smith, 1997; Stancalie et al., 2006; Wang, 2004; Wang et al., 2002). The pre and post flood Landsat 7 TM images were used to identify water and non-water features to identify flooded areas (Wang et al., 2002). Flooded areas and damaged buildings due to the 2011 Japan tsunami were identified based on the difference of backscattering coefficients from the pre and post tsunami TerraSAR-X intensity images (Mori et al., 2011). Flood monitoring in Bangladesh is done using a supervised classification technique using RADARSAT data (Hoque et al., 2011). A recent paper proposed a hybrid neuro fuzzy classifier known as Fuzzy Kohonen Local Information C-Means (FKLICM) Clustering for Remote Sensing Imagery (Singh et al., 2014). FKLICM is a hybridization of KCN with FLICM. Celik and Lee commented and proved that due to the design of the objective function of FLICM, the local minimizers do not converge to the correct local minima (Celik and Lee, 2013). The objective function of FKLICM is the same as that of FLICM and after conducting a thorough evaluation of the method it is revealed that the limitation associated with FLICM prevailed in FKLICM too. The proposed classifier is a hybridization of Kohonen Clustering Network (KCN) with FCM-σ clustering algorithm. It overcomes the limitations of FKLICM. The advantages of HKFCM-σ have been discussed later. In September 2014, heavy rainfall occurred in Jammu and Kashmir area which caused disastrous flooding and landslides all over the area including Jammu and Kashmir and adjoining areas of Pakistan also. In this paper, a method for identification of flooded areas using the proposed novel HKFCM-σ classifier is presented. The method classifies the pre and post flooding images using HKFCM-σ into different land cover classes and then using post classification comparison a classified change map is obtained which shows the flooded areas. The method is applied on areas of Kashmir to identify the flooding that occurred in September 2014.

2. Site description and satellite data used

Pre and Post flooding Landsat 8 Operational Land Imager (OLI) images acquired on 25th August 2014 and 10th September 2014 respectively are used for the study [http://glovis.usgs.gov]. Landsat 8 is an earth observation satellite launched on February 11, 2013. Landsat 8 Operational Land Imager (OLI) images consist of eleven spectral bands with a spatial resolution of 15 m for PAN band, 30 m for Bands 1–7 and 9. The band characteristics of Landsat 8 are given Table 1.

The study area covers around 7578.3814 sq km area of parts of Jammu and Kashmir including Handwara, Bandipora, Sopore, Pattan, Srinagar, Pahalgam, Poonch and other nearby areas. Fig. 1 shows the location of the study area. The geographical coordinates of Jammu and Kashmir are 33.4500° N, 76.2400° E. The false color composite pre and post flooding images are shown in Fig. 2.

3. Methodology

The flow chart of the proposed method is shown in Fig. 3. These steps are as follows:

3.1. Image preprocessing

The input images are preprocessed to obtain accurate results and remove any sort of distortions. The study area covers mountainous regions and therefore there is brightness difference due to image acquisition under different sun illumination conditions. Thus to compensate for this difference, the Top of Atmospheric (ToA) reflectance of the images is computed. Quantitative comparison of multi-temporal images requires conversion of DN values to reflectance (Lu et al., 2008). The conversion is done to overcome the brightness difference due

Table 1 Band Characteristics of Landsat 8 OLI.

Bands	Wavelength (m)	Resolution
Band 1 – Coastal aerosol	0.43–0.45	30
Band 2 – Blue	0.45–0.51	30
Band 3 – Green	0.53–0.59	30
Band 4 – Red	0.64–0.67	30
Band 5 – Near Infrared (NIR)	0.85–0.88	30
Band 6 – SWIR 1	1.57–1.65	30
Band 7 – SWIR 2	2.11–2.29	30
Band 8 – Panchromatic	0.50–0.68	15
Band 9 – Cirrus	1.36–1.38	30
Band 10 – Thermal Infrared (TIRS) 1	10.60–11.19	100 * (30)
Band 11 – Thermal Infrared (TIRS) 2	11.50–12.51	100 * (30)

Please cite this article in press as: Singh, K.K., Singh, A., , Identification of flooded area from satellite images using Hybrid Kohonen Fuzzy C-Means sigma classifier, Egypt. J. Remote Sensing Space Sci. (2016), http://dx.doi.org/10.1016/j.ejrs.2016.04.003

Figure 1 Location of the study area.

to image acquisition under different sun illumination conditions should be compensated. Secondly, the difference in DN values due to the seasonal adjustment of sensor parameters by the data provider. Thus, the DN values are converted into the top of atmosphere reflectance (ρ_{TOA}) to resolve the above mentioned issues.

3.2. Spectral indices

Spectral indices are used for highlighting a particular type of land cover like NDVI is used for vegetation, NDBI for built up areas and NDWI for water. In the proposed method, spectral indices are used for training of the hybrid Kohonen FCM-σ classifier. The study area is classified into four classes, vegetation, water, snow and bare land. Thus those spectral indices which highlight these land cover types are used for training. NDVI, NDWI, PC-1 and NDBI are derived from the different wavelength bands. In NDVI, the vegetated area pixels have higher values as compared to other features. Similarly NDWI and NDBI highlight the water and Bare land areas respectively. NDVI is used to highlight vegetated areas using visible and near infrared bands. Dense vegetation absorbs visible light and reflects near infrared light whereas sparse vegetation reflects visible light and absorbs near infrared light.

The NDVI image is computed using the following Eq. (1)

$$NDVI = \frac{\psi_{nir} - \psi_{red}}{\psi_{nir} + \psi_{red}} \quad (1)$$

NDWI is used to highlight the water bodies and snow covered areas in satellite imageries. NDWI makes use of green and NIR band of the electromagnetic spectrum to highlight water.

Please cite this article in press as: Singh, K.K., Singh, A., , Identification of flooded area from satellite images using Hybrid Kohonen Fuzzy C-Means sigma classifier, Egypt. J. Remote Sensing Space Sci. (2016), http://dx.doi.org/10.1016/j.ejrs.2016.04.003

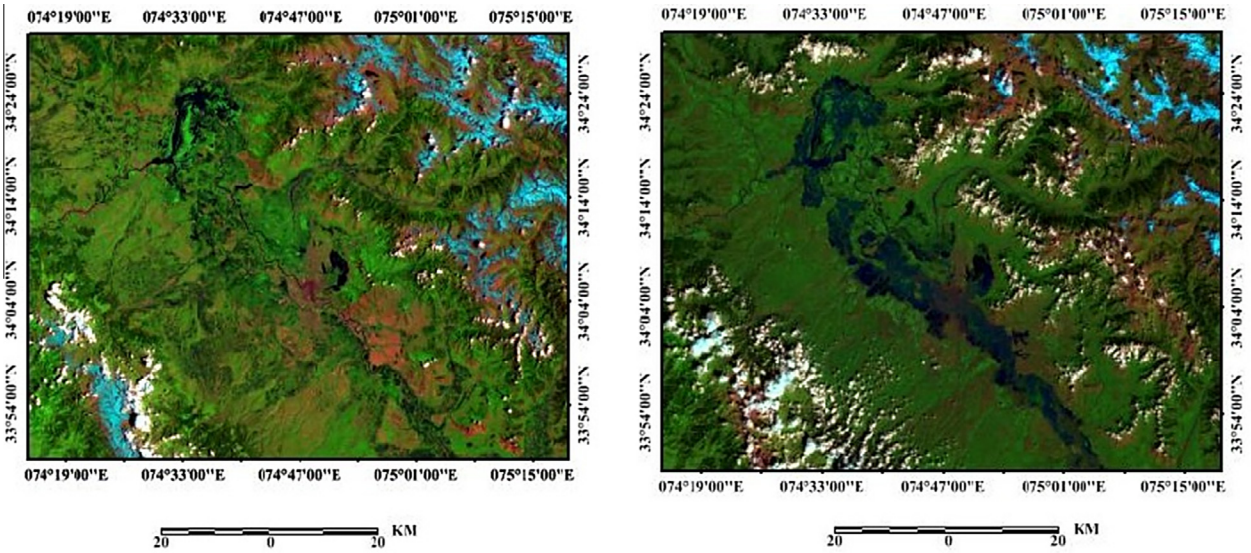

Figure 2 False Natural Color Composite (R: SWIR, G: NIR, B: Green) Pre and Post flooding.

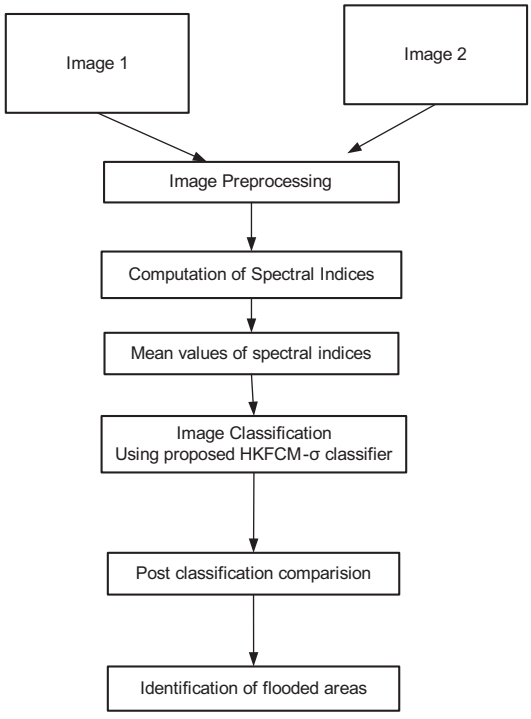

Figure 3 Flowchart of the proposed method.

Water features have positive values of NDWI whereas vegetation and soil have NDWI values equal to or less than zero (McFeeters, 1996).

$$NDWI = \frac{\psi_{green} - \psi_{nir}}{\psi_{green} + \psi_{nir}} \tag{2}$$

NDBI is used for highlighting the built up areas and barren lands have high increase in reflectance values from MIR band to NIR band. The speed at which the increase in reflectance value occurs is greater than any other land cover type.

$$NDBI = \frac{\psi_{mir} - \psi_{nir}}{\psi_{mir} + \psi_{nir}} \tag{3}$$

where $\psi_{nir}, \psi_{red}, \psi_{mir}, \psi_{green}$ represent the near infrared, red, mid infrared and green band respectively. PCA is a statistical technique that transforms a multivariate data set of intercorrelated variables into a data set of new uncorrelated linear combinations of the original variables. The PCA approach involves computation of covariance matrix, eigen values and vectors, Principal components. The first component of PCA commonly termed as PC-1, is used for highlighting the cloud cover. These images are normalized into (0, 255) using Eq. (4) for determining the optimal threshold value,

$$x(i,j) = \frac{(I(i,j) - \min(I))}{\max(I) - \min(I)} \times 255 \tag{4}$$

where $x(i, j)$ corresponds to the pixels of the normalized image X, I is the input image, min(.) and max(.) represent the maximum and minimum pixel value of the input image. In pre flooding image, vegetated areas have NDVI values greater than 155, water has NDWI values in the range 110–155, and urban areas have NDBI values greater than 160 and clouds have values greater than 130 in the PC-1 image. In post flooding scene, the vegetated areas have NDVI values greater than 176, clouds have PC-1 values greater than 105, water pixels have NDWI values in the range 120 and 170 and urban area have NDBI values greater than 180. The spectral indices are shown in Fig. 4.

3.3. Hybrid Kohonen FCM-σ

Hybrid Kohonen FCM-σ classifier is a neuro fuzzy classifier is a hybridization of the Kohonen Clustering Network (KCN) (Kohonen, 2012) and FCM-σ (Tsai and Lin, 2011). The KCN is the simplest neural network, without any activation function and hidden layer. The network consists of only two layers, i.e., input layer and output layer. The neuron with minimum Euclidean distance from the input vector is the winner. The weight of the winner and its predefined neighbors are updated using a learning rule. KCN is sequential in nature and is a hard clustering network and thus is not suited well for image classification problems as it is unable to handle

Please cite this article in press as: Singh, K.K., Singh, A., , Identification of flooded area from satellite images using Hybrid Kohonen Fuzzy C-Means sigma classifier, Egypt. J. Remote Sensing Space Sci. (2016), http://dx.doi.org/10.1016/j.ejrs.2016.04.003

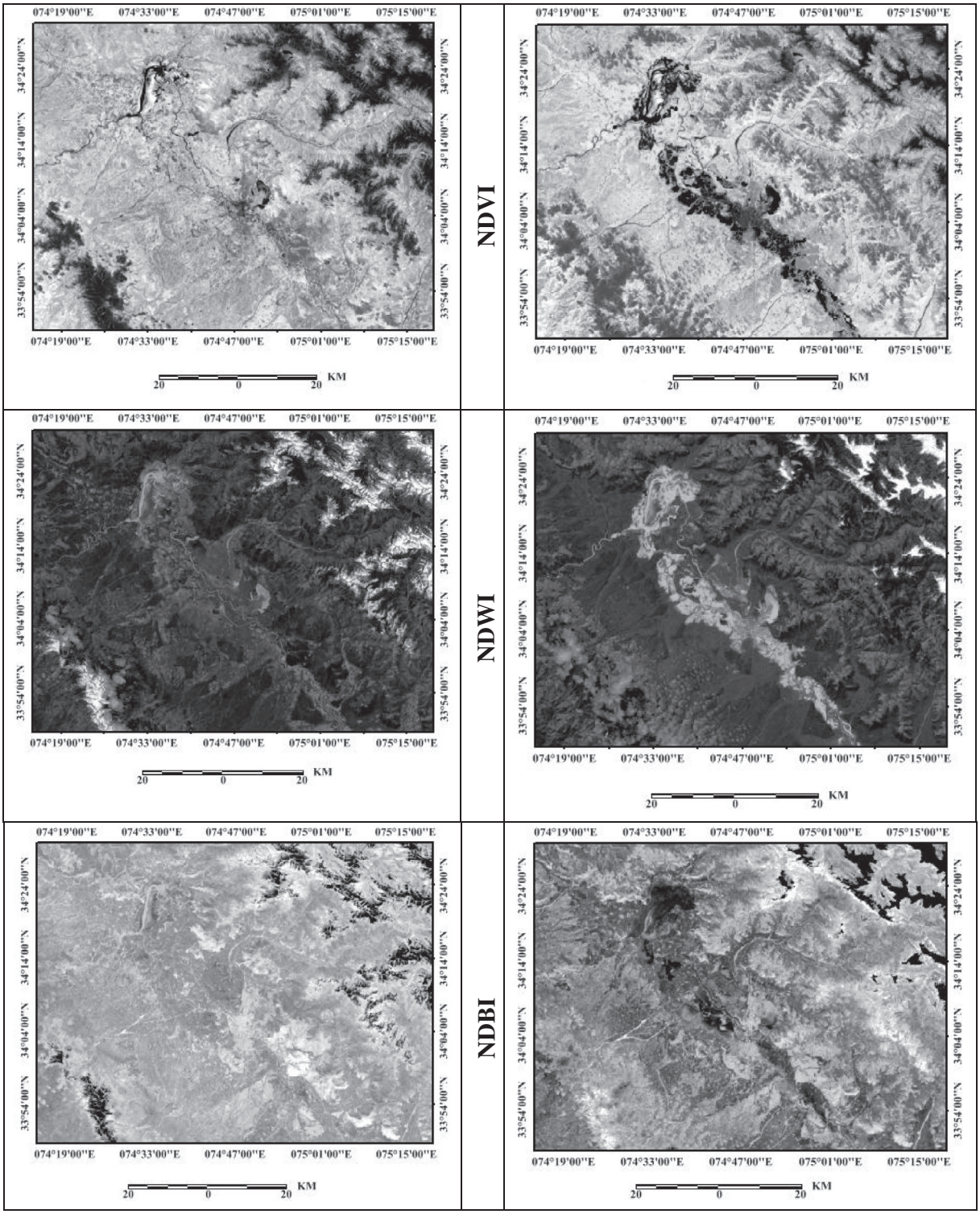

Figure 4 Response of various spectral indices applied on (a) pre flooding image (b) post flooding image.

mixed pixel problem. But its simplicity makes it a popular choice, thus to incorporate fuzzy features in KCN it is hybridized with FCM-σ clustering algorithm. FCM-σ is an improvement of the conventional FCM algorithm. The limitation with conventional FCM is that it only considers the Euclidean distances between individual points and the cluster centers. It ignores the intra cluster distances which degrades the performance of the clustering. FCM-σ overcomes this limitation by considering both inter cluster as well as intra cluster distances. It partitions a collection of data points into c fuzzy clusters. Each cluster has a cluster center. The cluster centers are such that they minimize the value of the objective function. FCM-σ employs fuzzy partitioning, where a point can belong to several clusters with degrees of membership. A membership

Please cite this article in press as: Singh, K.K., Singh, A., , Identification of flooded area from satellite images using Hybrid Kohonen Fuzzy C-Means sigma classifier, Egypt. J. Remote Sensing Space Sci. (2016), http://dx.doi.org/10.1016/j.ejrs.2016.04.003

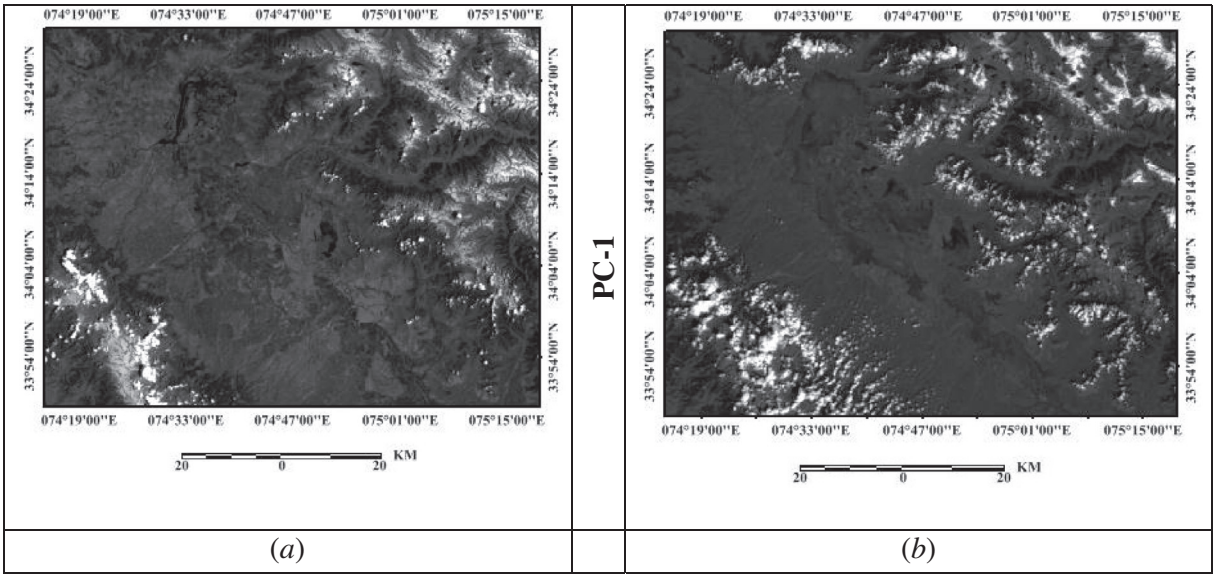

Fig. 4 (*continued*)

matrix is made which has elements in the range (0, 1) representing fuzzy partitioning. A point's total membership of all clusters, however, must always be equal to unity to maintain the properties of the membership matrix. The hybridization of these two combines the advantages of both a neural system and a fuzzy system. HKFCM-σ is a neuro fuzzy classifier that overcomes the limitations of KCN and FCM-σ On the other hand it has the advantages of both the systems.

The algorithm of the proposed HKFCM-σ algorithm is as follows:

Step 1. Initialize the cluster center $\xi_i (2 \leqslant i \leqslant c)$, the threshold $\varepsilon(\varepsilon > 0)$ and topological neighborhood parameters. Set $t = 1$, maximum iteration limit t_{max} and $\eta > 1$. The fuzziness index η_t is updated by

$$\eta_t = \eta + \frac{t(\eta - 1)}{t_{max}} \text{ for } 1 < t \leqslant t_{max} \text{ and } \eta > 1 \tag{5}$$

Step 2. Calculate fuzzy membership matrix u_{ik} and learning rate $\gamma_{ik,t}$ using Eqs. (6) and (8).

$$u_{ik} = \left(\sum_{l=1}^{c} \left(\frac{\partial_{ik}^2}{\partial_{lk}^2} \right)^{1/(\eta_t - 1)} \right)^{-1} \text{ for } 1 \leqslant i \leqslant c \text{ and } 1 \leqslant k \leqslant n \tag{6}$$

where

$$\partial_{ik}^2 = \frac{\|\xi_i - I_k^2\|}{\sigma_i} \tag{7}$$

and $\sigma_i = \frac{\sum_{k=1}^{n} u_{ik}^{\eta_t} \|\xi_i - I_k^2\|}{\sum_{k=1}^{n} u_{ik}^{\eta_t}}$ the membership matrix $U = [u_{ik}]$, represents a fuzzy c-partition matrix constrained by the probabilistic conditions $0 \leqslant u_{ik} \leqslant 1$, and $\sum_{i=1}^{c} u_{ik} = 1 \forall i = 1, .., c$..The learning rate $\lambda_{ik,t}$ of the ikth neuron for tth iteration is given by Eq. (8).

$$\lambda_{ik,t} = (u_{ik})^{\eta_t} \tag{8}$$

Step 3. The weight of the output neuron is updated using Eq. (9).

$$\xi_{i,t} = \xi_{i,t-1} + \sum_{k=1}^{n} \lambda_{ik,t} (I_k - \xi_{i,t-1}) / \sum_{s=1}^{n} \lambda_{is,t} \tag{9}$$

Step 4. Update the learning rate $\lambda_{ik,t}$.

Step 5. $t = t + 1 for 1 \leqslant t \leqslant t_{max}$.

Step 6. If $\|\xi_{1,t} - \xi_{1,t-1}\| > \varepsilon$ then go to step 2, otherwise go to step 7.

Step 7. Output the final clustered image by assigning the pixel I_k to the class c with highest membership value, i.e., when the algorithm has converged, a defuzzification process takes place in order to convert the fuzzy partition matrix U to a crisp partition. The maximum membership procedure is the most important method that has been developed to defuzzify the partition matrix U. The procedure assigns the pixel k to the class with the highest membership

$$C_k = arg_i \{\max\{u_{ik}\}\}, i = 1, 2, \ldots, c$$

It is used to convert the fuzzy image achieved by the proposed algorithm to the crisp segmented image.

The following advantages of HKFCM-σ have been observed

1. Sequential Data feeds: KCN is sequential in nature, its result depends on the sequence of data feed whereas HKFCM-σ updates the centers after each training epoch. Thus, HKFCM-σ works parallel and is independent of the feeding sequence.
2. Complexity: HKFCM-σ is less complex as compared to KCN and due to its parallel nature it has a complexity of $O(t^*)$.

Please cite this article in press as: Singh, K.K., Singh, A., , Identification of flooded area from satellite images using Hybrid Kohonen Fuzzy C-Means sigma classifier, Egypt. J. Remote Sensing Space Sci. (2016), http://dx.doi.org/10.1016/j.ejrs.2016.04.003

3. Termination: KCN always iterated to its maximum iteration number. However due to the stopping criteria used in HKFCM-σ it stopped when the optimal result is obtained making it faster.

The training of the classifier is done from the mean values of the spectral indices derived in Section 3.2. This classifier is used to classify the pre and post flooding images into four classes namely vegetation, water, urban area, snow and water as shown in Fig. 5(a) and (b).

4. Change detection

Post classification comparison method is applied on the pre and post classified images to obtain a classified change map which highlights the flooded area. The result of change detection is shown in Fig. 5(c). For p classes a total of $p * (p-1)$ change classes are possible. The pre and post images are classified into four classes, thus total twelve change classes are possible. But since the aim is to detect flooded areas thus all those change classes in which any class is changed to water class are merged into one class and named as flooded area class which shows the flooded areas. The results show that the original water bodies spanned over an area of 100.2438 sq km and after flooding this area increased to 334.2456 sq. km. Thus, the total flooded area is approximately 234 sq. km.

5. Accuracy assessment

The performance evaluation of the proposed classifier is done using accuracy assessment of the classifier. It gives an insight of the detected change results. One of commonly used methods is to apply an error matrix which can be used to compute a number of assessment elements like overall accuracy and kappa coefficient (Foody, 2002; Congalton and Green, 2008; Congalton, 1991). One of the most important task in accuracy assessment is selection of sampling strategy for collection of ground points. The commonly used approach is to use the training pixels that are used to train the classifier for accuracy assessment. But the limitation with this approach is that the training pixels are not random and also they are influenced by the analyst's knowledge about the location of different classes. An alternative to this is random selection of points but when points are selected randomly certain small classes are ignored. Thus, stratified random technique is used as it is not biased and also the selection of points is random covering

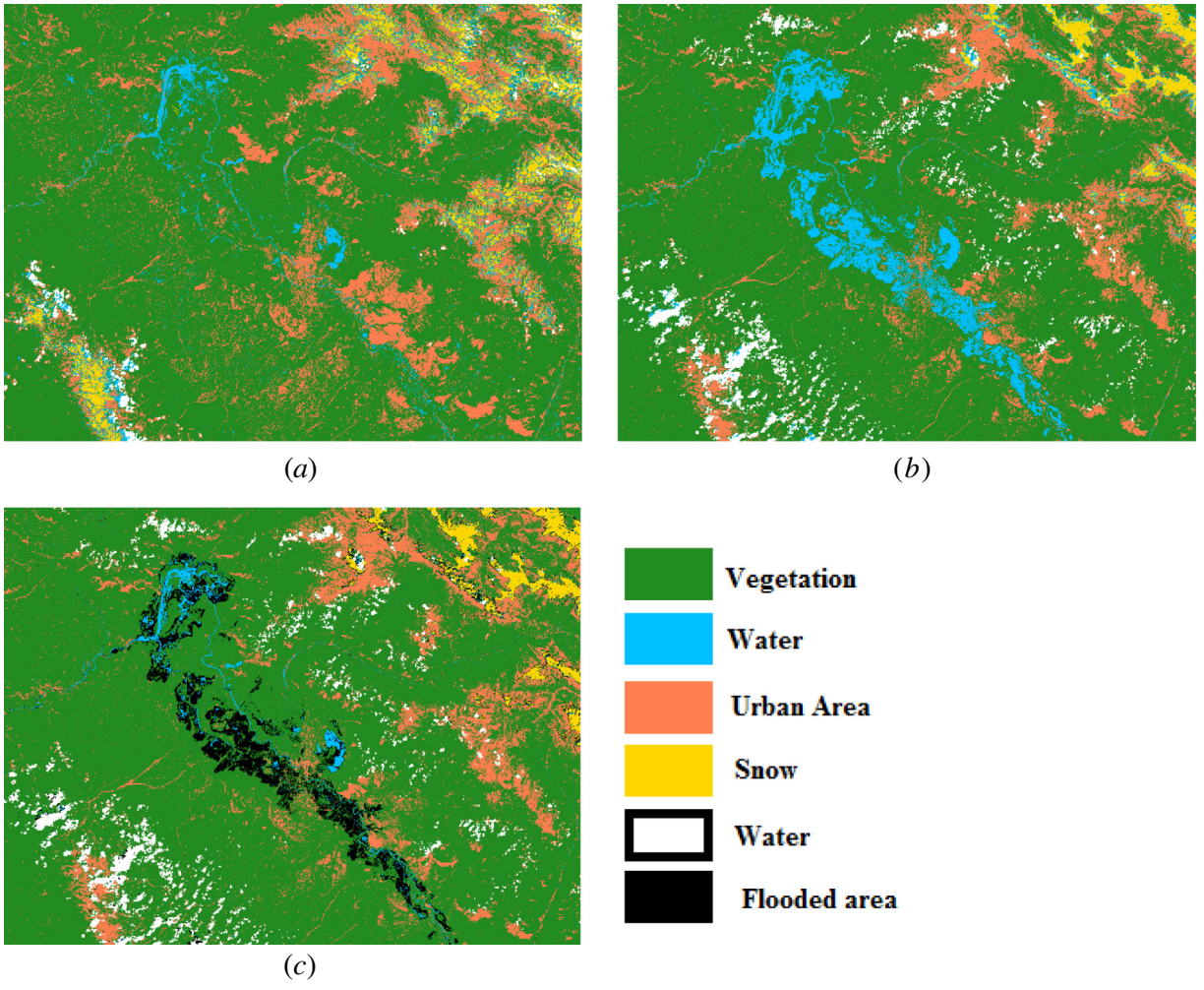

Figure 5 (a) Pre flooding classified image (b) Post flooding classified image (c) Classified change map.

Table 2 Error matrix for pre flooding image.

Reference data	Water	Cloud	Urban	Vegetation	Snow	Total
Water	14	0	0	0	1	15
Cloud	0	7	1	0	0	8
Urban	1	1	41	2	0	45
Vegetation	1	0	4	163	2	170
Snow	1	0	0	0	17	18
Total	17	8	46	165	20	256

Table 3 Accuracy Results for pre flooding image.

Class name	Producers accuracy	User's accuracy	Conditional kappa
Water	82.35	93.33	0.9286
Cloud	87.50	87.50	0.8710
Urban	89.13	91.11	0.8916
Vegetation	98.79	95.88	0.8842
Snow	85.00	94.44	0.9397

Overall accuracy: 94.53 overall kappa: 0.8968.

Table 4 Error matrix for post flooding image.

Reference data	Water	Cloud	Urban	Vegetation	Snow	Total
Water	18	0	0	0	1	19
Cloud	0	12	1	0	0	13
Urban	1	1	29	1	0	32
Vegetation	2	0	3	174	3	182
Snow	1	0	0	0	9	10
Total	22	13	33	175	13	256

Table 5 Accuracy results for post flooding image.

Class name	Producers accuracy	User's accuracy	Conditional kappa
Water	81.82	94.74	0.9424
Cloud	92.31	92.31	0.9190
Urban	87.88	90.63	0.8924
Vegetation	99.43	95.60	0.8611
Snow	69.23	90.00	0.8947

Overall accuracy: 94.53 overall kappa: 0.8877.

Table 6 Accuracy and kappa.

Method	Overall accuracy	Kappa
FCM (Bezdek, 2013)	91.80	0.8431
GIFP-FCM (Zhu et al., 2009)	92.33	0.8652
FCM-σ	93.37	0.8794
HKFCM-σ	94.53	0.8877

all classes. In this paper, stratified random technique from ERDAS™ software is used for accuracy assessment. The images are classified in Matlab R2013a and thus the geotiffwrite function of Matlab R2013a, which writes a georeferenced image is used. These classified images can be used in ERDAS™ for accuracy assessment. Confusion matrix is used for analyzing the results analytically as well as descriptively. The various assessment elements that are used here are overall accuracy, kappa coefficient, producer's accuracy and user's accuracy. A total of 256 reference points were chosen using stratified random sampling. The confusion matrices and the various assessment elements for both pre and post tsunami classified images are shown in Tables 2–5 respectively. The overall accuracy is 94.53% for both pre and post flooding images. The value of kappa coefficient is 0.8698 for pre flooding and 0.8877 for post flooding image. The high overall accuracy and the value of kappa coefficient show that the results obtained are quite satisfactory. Accuracy and kappa coefficient values of the three methods are listed in Table 6. It is observed that Hybrid Kohonen Fuzzy C-Means sigma (HKFCM-σ) classifier has highest overall accuracy and highest value of kappa coefficient, conforming that the proposed method outperforms the other two.

Accuracy and kappa coefficient values of the three methods are listed in Table 6. It is observed that Hybrid Kohonen Fuzzy C-Means sigma (HKFCM-σ) classifier has the highest overall accuracy and highest value of kappa coefficient, conforming that the proposed method outperforms the other two.

6. Conclusion

This paper presents, a novel neuro fuzzy classifier Hybrid Kohonen FCM-σ. The proposed classifier is a hybridization of Kohonen Clustering Network and FCM-σ clustering algorithm. It has the features of both a neural network as well as a fuzzy system. Thus, the proposed classifier is parallel, efficient, fast and less complex classifier. These classifier is applied on pre and post flooding Landsat 8 OLI images of Kashmir area to detect the flooding that occurred in September 2014 in this area. The classified change map is created using post classification comparison method. The change map shows that about 234 sq. km area was flooded. The results were analyzed both quantitatively as well as qualitatively and it is observed that the results produced are effective and efficient. Accuracy assessment shows that the proposed method has high accuracy and can be used for disaster management activities.

Conflict of interest

No Conflict of Interest.

References

Barton, I.J., Bathols, J.M., 1989. Monitoring floods with AVHRR. Remote Sens. Environ. 30 (1), 89–94.

Bezdek, J.C., 2013. Pattern Recognition with Fuzzy Objective Function Algorithms. Springer Science & Business Media.

Brakenridge, G.R., Anderson, E., Nghiem, S.V., Caquard, S., Shabaneh, T.B., 2003a. Flood Warnings, Flood Disaster Assessments, and Flood Hazard Reduction: The Roles of Orbital Remote Sensing. Jet Propulsion Laboratory, National Aeronautics and Space Administration, Pasadena, CA, p. 869.

Brakenridge, R., Carlos, H., Anderson, E.K., 2003b. River gaging reaches: a strategy for MODIS-based river monitoring. In: International Symposium on Remote Sensing. International Society for Optics and Photonics, pp. 479–486.

Celik, T., Lee, H.K., 2013. Comments on "A Robust Fuzzy Local Information C-Means Clustering Algorithm". IEEE Trans. Image Proc. 22 (3), 1258–1261.

Congalton, R.G., 1991. A review of assessing the accuracy of classifications of remotely sensed data. Remote Sens. Environ. 37 (1), 35–46.

Congalton, R.G., Green, K., 2008. Assessing the Accuracy of Remotely Sensed Data: Principles and Practices. CRC Press.

Foody, G.M., 2002. Status of land cover classification accuracy assessment. Remote Sens. Environ. 80 (1), 185–201.

France, M.J., Hedges, P.D., 1986. A hydrological comparison of Landsat TM, Landsat MSS and black & white aerial photography. In: Remote sensing for resources development and environmental management. International symposium. 7, pp. 717–720.

Gale, S.J., Bainbridge, S., 1994. Megafloods in inland eastern Australia, April 1990. Z. Geomorphol. 38 (1), 1–11.

Hoque, R., Nakayama, D., Matsuyama, H., Matsumoto, J., 2011. Flood monitoring, mapping and assessing capabilities using RADARSAT remote sensing, GIS and ground data for Bangladesh. Nat. Hazards 57 (2), 525–548.

Jensen, J.R., Hodgson, M.E., Christensen, E., Mackey Jr., H.E., Tinney, L.R., Sharitz, R., 1985. Remote Sensing Inland Wetlands: A Multispectral Approach (No. DP-MS-85-68). South Carolina Univ., Columbia (USA). Dept. of Geography; Du..

Kohonen, T., 2012. Self-organization and associative memory (vol. 8). Springer Science & Business Media.

Lu, D., Batistella, M., Moran, E., 2008. Integration of Landsat TM and SPOT HRG images for vegetation change detection in the Brazilian Amazon. Photogramm. Eng. Remote Sens. 74 (4), 421.

Manjunath, A.S., Jain, D.S., Kumar, S.R., Anjaneyulu, R.V.G., 2007. Role of satellite communication and remote sensing in rural development. IETE Tech. Rev. 24 (4), 215–224.

McFeeters, S.K., 1996. The use of the Normalized Difference Water Index (NDWI) in the delineation of open water features. Int. J. Remote Sens. 17 (7), 1425–1432.

Mori, N., Takahashi, T., Yasuda, T., Yanagisawa, H., 2011. Survey of 2011 Tohoku earthquake tsunami inundation and run-up. Geophys. Res. Lett. 38 (7).

Rasid, H., Pramanik, M.A.H., 1993. Areal extent of the 1988 flood in Bangladesh: How much did the satellite imagery show? Nat. Hazards 8 (2), 189–200.

Sandholt, I., Nyborg, L., Fog, B., Lô, M., Bocoum, O., Rasmussen, K., 2003. Remote sensing techniques for flood monitoring in the Senegal River Valley. Geografisk Tidsskrift-Danish J. Geogr. 103 (1), 71–81.

Singh, K.K., Nigam, M.J., Pal, K., Mehrotra, A., 2014. A fuzzy kohonen local information C-means clustering for remote sensing imagery. IETE Tech. Rev. 31 (1), 75–81.

Smith, L.C., 1997. Satellite remote sensing of river inundation area, stage, and discharge: a review. Hydrol. Process. 11 (10), 1427–1439.

Stancalie, G., Diamandi, A., Corbus, C., Catana, S., 2006. Application of EO Data In Flood Forecasting For The Crisuri Basin, Romania. In: Flood Risk Management: Hazards, Vulnerability and Mitigation Measures. Springer, Netherlands, pp. 101–113.

Tsai, D.M., Lin, C.C., 2011. Fuzzy C-means based clustering for linearly and nonlinearly separable data. Pattern Recogn. 44 (8), 1750–1760.

Wang, Y., 2004. Using Landsat 7 TM data acquired days after a flood event to delineate the maximum flood extent on a coastal floodplain. Int. J. Remote Sens. 25 (5), 959–974.

Wang, Y., Colby, J.D., Mulcahy, K.A., 2002. An efficient method for mapping flood extent in a coastal floodplain using Landsat TM and DEM data. Int. J. Remote Sens. 23 (18), 3681–3696.

Watson, J.P., 1991. A visual interpretation of a Landsat mosaic of the Okavango Delta and surrounding area. Remote Sens. Environ. 35 (1), 1–9.

Zhu, L., Chung, F.L., Wang, S., 2009. Generalized fuzzy c-means clustering algorithm with improved fuzzy partitions. IEEE Trans. Syst. Man Cybern. Part B Cybern. 39 (3), 578–591.

Please cite this article in press as: Singh, K.K., Singh, A., , Identification of flooded area from satellite images using Hybrid Kohonen Fuzzy C-Means sigma classifier, Egypt. J. Remote Sensing Space Sci. (2016), http://dx.doi.org/10.1016/j.ejrs.2016.04.003